



## Fabrication of patterned CdS/TiO<sub>2</sub> heterojunction by wettability template-assisted electrodeposition

Yuekun Lai<sup>a,b</sup>, Zequan Lin<sup>a</sup>, Zhong Chen<sup>b</sup>, Jianying Huang<sup>c</sup>, Changjian Lin<sup>a,\*</sup>

<sup>a</sup> State Key Laboratory of Physical Chemistry of Solid Surfaces, and College of Chemistry and Chemical Engineering, Xiamen University, Xiamen 361005, China

<sup>b</sup> School of Materials Science and Engineering, Nanyang Technological University, 50 Nanyang Avenue, Singapore 639798, Singapore

<sup>c</sup> Fujian Institute of Research on the Structure of Matter, Chinese Academy of Sciences, Fuzhou 350002, China

### ARTICLE INFO

#### Article history:

Received 6 February 2010

Accepted 8 March 2010

Available online 15 March 2010

#### Keywords:

TiO<sub>2</sub> nanotube

CdS nanosphere

Wettability micropattern

Electrodeposition

Semiconductors

Nanomaterials

### ABSTRACT

A wettability template-assisted process was applied to selectively deposit cadmium sulfide (CdS) nanospheres on TiO<sub>2</sub> nanotube layers to form uniformly coupled CdS/TiO<sub>2</sub> semiconductor heterojunction micropatterns. The effect of deposition time on the size and morphology of the as-prepared CdS/TiO<sub>2</sub> array patterns was investigated. It is shown that the CdS nanocrystals with a highly ordered, hierarchically porous structure in nano-micro dual scales could be selectively grown within the superhydrophilic regions. The patterned CdS/TiO<sub>2</sub> heterojunctions have demonstrated enhanced photo-response under both UV and visible light irradiation. This novel template patterning technique, which is based on wettability contrast, can be applied to a broad range of technological areas, such as sensor arrays and optoelectronic devices.

© 2010 Elsevier B.V. All rights reserved.

### 1. Introduction

In recent years, patterned thin films have received considerable attentions due to their interesting properties for a range of applications, such as optoelectronic devices, magnetic storage media, gas sensors, and microfluidic systems [1–7]. Compared to the conventional thin film technology, such as physical vapor deposition, chemical vapor deposition and sputtering, solution-based deposition method is becoming popular for the fabrication of patterning films due to the low temperature process under ambient environment, less energy and time consumption, and easier control of the experimental parameters [8–10]. Although photolithographic technique is excellent for preparing submicro-sized template for patterning in solution, it is a complex multi-step process and needs to remove part of the film and the photoresist used. Direct and selective assembly of nanostructured materials from precursors paves a new avenue for the fabrication of electronic optical microdevices. Wettability of solid surfaces is a very important property of solid surface. Surfaces with extreme wetting properties, e.g. superhydrophilic and superhydrophobic, can be prepared by introducing certain rough structures on the originally “common” hydrophilic and hydrophobic surfaces. Superhydrophilicity and superhydrophobicity are defined based on the conventional water contact angle experiment. If the contact angle is smaller than 5°, the surface is said to be superhydrophilic.

Superhydrophobic refers to surface with contact angle greater than 150°. The great difference in contact angle of the two extreme cases provides a potentially powerful and economical platform to directly and precisely construct patterned nanostructures in aqueous solution. So far, only a few reports have been available on the fabrication and application of superhydrophilic–superhydrophobic patterning [11–13].

In this paper, we demonstrate using a novel synthetic process to prepare patterned semiconductor heterojunction structures. The novelty of the present work is the discovery that position-controlled film growth on a solid substrate can be accomplished by using extreme wettability enhanced by rough structure to induce or suppress the nucleation and growth of CdS crystals. The enhanced photoelectrochemical performance of the coupled CdS/TiO<sub>2</sub> heterojunction films has also been described and discussed.

### 2. Experimental

#### 2.1. Fabrication of superhydrophilic–superhydrophobic template on TiO<sub>2</sub> nanotube films

The preparation of superhydrophobic TiO<sub>2</sub> nanotube films followed a similar method described previously [14,15]. Titanium sheets (99.5%) were electrochemically anodized in 0.5 wt.% HF solution under 20 V. The amorphous TiO<sub>2</sub> nanotube films were calcined at 450 °C for 2 h to form anatase phase and then treated with a methanolic solution of hydrolyzed 1 wt.% 1H,1H,2H,2H-perfluorooctyl-triethoxysilane (PTES, Degussa Co., Ltd.) for an hour and

\* Corresponding author.

E-mail address: [cjlin@xmu.edu.cn](mailto:cjlin@xmu.edu.cn) (C. Lin).

subsequently heated at 140 °C for an hour. The obtained superhydrophobic film was selectively exposed to UV light through a photomask to obtain the superhydrophilic–superhydrophobic pattern.

## 2.2. Electrodeposition of CdS micropattern on TiO<sub>2</sub> nanotube film

Successful formation of CdS patterns on the TiO<sub>2</sub> nanotube surface with high resolution on the superhydrophilic–superhydrophobic template requires optimized synthesis parameters such as solution composition, reacting temperature, current density and deposition time. After a series of preliminary experiments, the clearly defined patterns were obtained in the reaction electrolyte solution containing 50 mM CdCl<sub>2</sub> and 10 mM Na<sub>2</sub>S<sub>2</sub>O<sub>3</sub>. The electrodeposited process was applied for the current density of 0.5 mA/cm<sup>2</sup> at 70 °C for a certain time.

## 2.3. Characterization of the coupled CdS/TiO<sub>2</sub> heterojunctions

The morphology of the couple CdS/TiO<sub>2</sub> micropatterns was observed by field-emission scanning electron microscope (FESEM, LEO-1530, Germany). The crystallinity of the samples was measured using an X-ray diffractometer with Cu K<sub>α</sub> radiation (XRD, Phillips X'pert-PRO PW3040, Netherlands). Photoelectrochemical measurements were carried out in 0.1 M Na<sub>2</sub>SO<sub>4</sub> using an LHX 150 Xe lamp, and an electrochemical cell with a quartz window. The active area of the working electrode surface was 1 × 1 cm<sup>2</sup>, and the light intensity on the electrode surface was about 100 mW/cm<sup>2</sup>. The photo-response

was measured in a three-electrode configuration with a platinum wire counter-electrode and a reference saturated calomel electrode (SCE) at zero bias.

## 3. Results and discussion

### 3.1. Micropattern characterization

Fig. 1 shows the typical SEM micrographs of the CdS nanosphere micropatterns after 3 min deposition on the superhydrophilic–superhydrophobic template of TiO<sub>2</sub> nanotube films. A clear and uniform pattern with high resolution can be found in Fig. 1a. The bright rectangular areas corresponded to the deposition of CdS nanosphere crystals on the superhydrophilic regions. The boundary between the CdS pattern and the surrounding superhydrophobic regions is clearly visible at a higher magnification (Fig. 1b). The dispersed CdS nanosphere crystals grew on the top of TiO<sub>2</sub> nanotube arrays within the rectangular superhydrophilic region (Fig. 1c). Most of the crystals were less than 90 nm in diameter due to the confinement by the inner diameter of nanotube, though a few larger spheres (~120 nm) were seen across neighboring tube openings. While on the superhydrophobic areas (Fig. 1d), there was almost no CdS crystal. The high growth selectivity was also confirmed by the EDS analysis, revealing that CdS spheres easily nucleate and grow on the hydroxyl groups (–OH) terminated regions (Fig. 1e), but not on the –CF<sub>3</sub> terminated areas (Fig. 1f). Since the difference of the water contact angle between the superhydrophilic and superhydrophobic regions is larger than 150°, electrolyte solution is preferentially

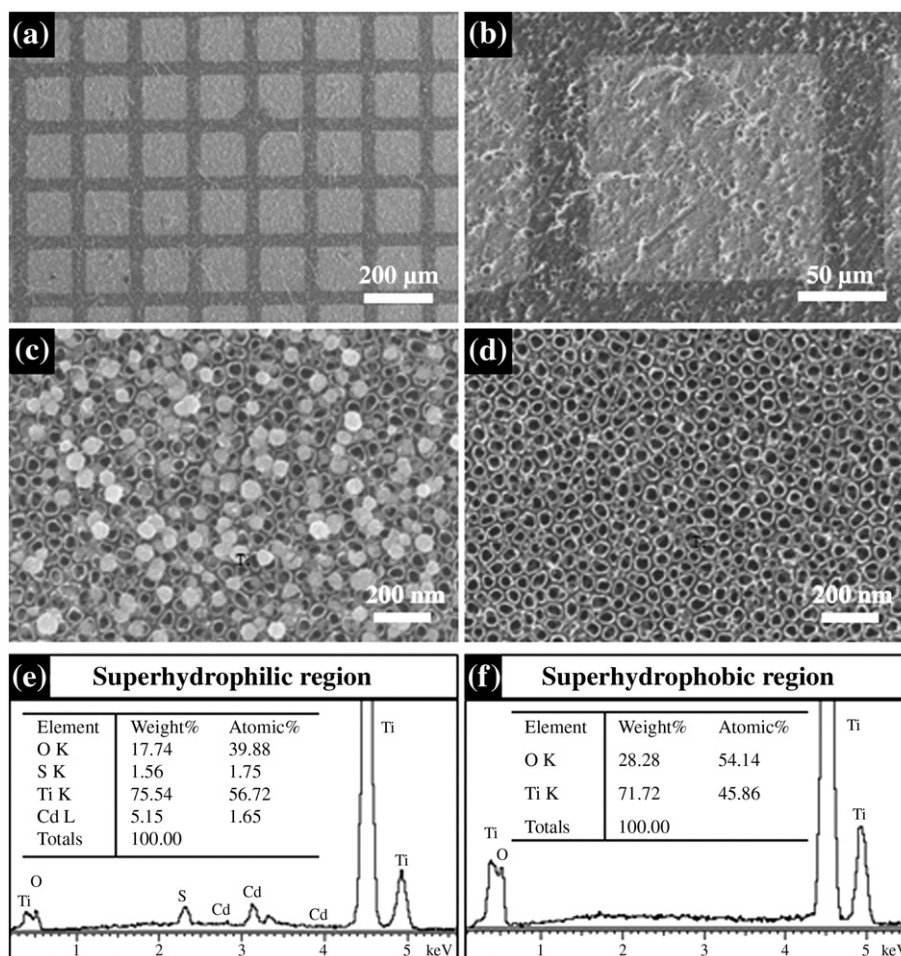


Fig. 1. Typical SEM images of the CdS micropattern (a,b), superhydrophilic region (c), and superhydrophobic region (d). EDX spectrum of the corresponding superhydrophilic (e) and superhydrophobic regions (f).

presented on the uniform superhydrophilic dots. No water droplets go to the neighboring superhydrophobic regions. Although a few CdS particles resulted from homogeneous precipitation attached onto superhydrophobic surface due to van der Waals interactions and gravity, they can be easily removed by ultrasonication (see [Supplementary data](#)). Therefore, a clear and well-defined CdS pattern in line with the dimensions of the superhydrophobic–superhydrophilic template has been obtained.

### 3.2. Effect of electrodeposition time

Fig. 2 shows representative top-view FESEM images of the CdS/TiO<sub>2</sub> heterojunction by electrodeposition for different times. With deposition for 2 min (Fig. 2a), the CdS nanosphere crystals with a diameter about 60 nm were sparsely dispersed in the superhydrophilic areas. Upon further increase in the deposition time to 3 min and 5 min (Fig. 2b and c), it was observed that CdS nanospheres were the predominant structural features. The average diameter of the CdS nanospheres increased to ~125 nm and 150 nm respectively. The electrodeposition time has a clear influence on the size of the CdS particles (see [Supplementary data](#)). Fig. 2d shows a comparison of XRD patterns of annealed TiO<sub>2</sub> nanotube array with or without CdS crystal deposition. It is apparent that the all annealed TiO<sub>2</sub> nanotube array samples exhibit the crystalline phase of anatase TiO<sub>2</sub>. The characteristic peaks (curves b–d) appeared at the diffraction angle of 24.9°, 26.6°, 28.2°, 43.9° and 47.9° can be assigned to the pure CdS hexagonal structure with crystal face of (100), (002), (101), (110) and (103). These characteristic peaks increase their intensity for longer deposition times, which indicates that the number of CdS nanospheres also grows up. These XRD results confirmed our SEM observation.

### 3.3. Photoelectrochemical activity

Fig. 3 shows the photocurrent spectra of the couple CdS/TiO<sub>2</sub> nanotube array electrode prepared under different electrodeposition times. It is apparent that the pure TiO<sub>2</sub> nanotube array samples have a photo-response wavelength lower than 400 nm due to its

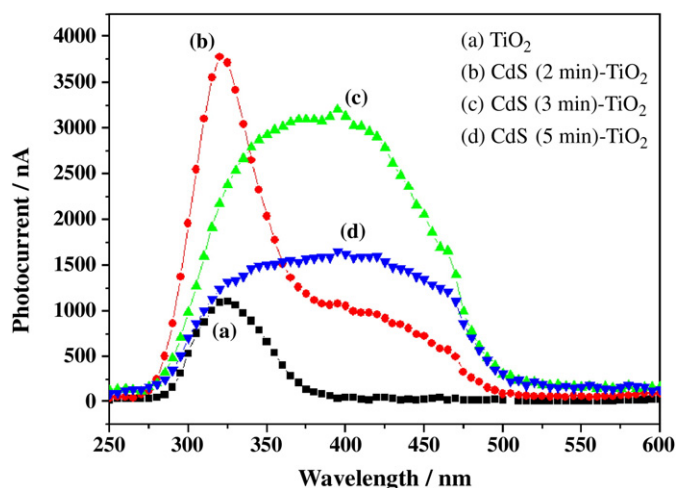


Fig. 3. Photocurrent spectra of micropatterned CdS film on TiO<sub>2</sub> nanotube array electrode. (a) Pure TiO<sub>2</sub>, (b) 2 min; (c) 3 min; and (d) 5 min.

band-gap of 3.2 eV (curve a). The decoration of CdS nanospheres with a smaller energy band-gap (2.4 eV) can significantly extend the photo-response range from 380 nm to about 500 nm. Moreover, the CdS modified TiO<sub>2</sub> nanotube array electrodes can also greatly increase the photocurrent response under UV light, especially for the samples obtained under 2 min electrodeposition (curve b), which thus would be the optimal deposition time. This is attributed to the uniform dispersed CdS nanospheres with suitable size decorated onto the TiO<sub>2</sub> nanotubes. This allows for more efficient electron transfer and lower electron-hole recombination rate which leads to enhanced light harvesting at the directly grown CdS/TiO<sub>2</sub> heterojunctions. With the increase of time (curve c and d), more CdS particles with bigger size started to randomly distribute on top of TiO<sub>2</sub> nanotube arrays. Such composite nanostructures would weaken the light absorption of the uniform CdS/TiO<sub>2</sub> heterojunction underlayer, which has resulted in a lower photocurrent in both UV and visible light region.

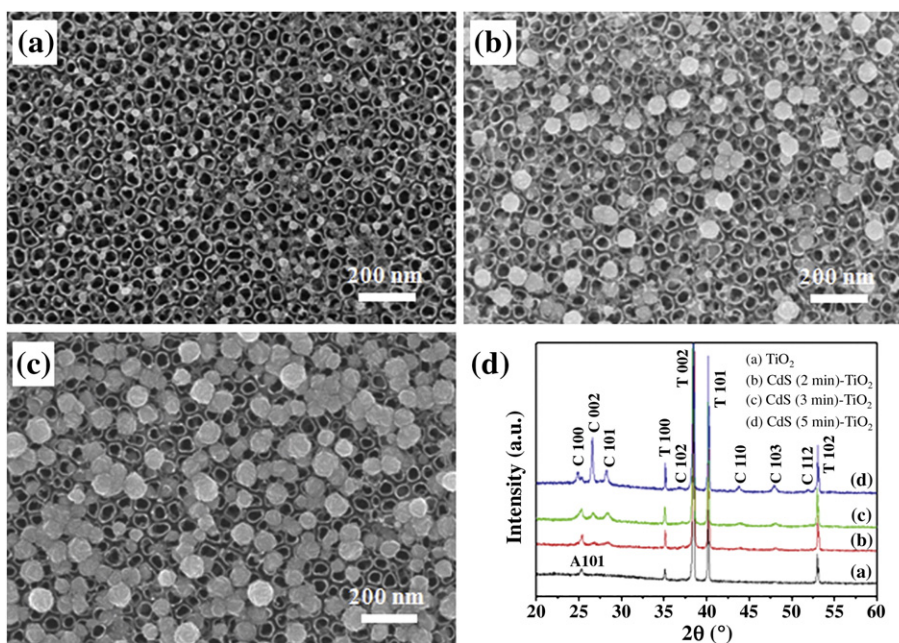


Fig. 2. SEM images of the CdS nanospheres selectively deposited in the predefined superhydrophilic regions on TiO<sub>2</sub> nanotube films by electrochemical deposition with a constant current density of 0.5 mA/cm<sup>2</sup> for different times. (a) 2 min; (b) 3 min; (c) 5 min; and (d) XRD spectra of the micropatterned CdS film under different deposition time. A, C and T represent anatase TiO<sub>2</sub>, CdS and titanium, respectively.

#### 4. Conclusions

In summary, we have demonstrated a successful application of wettability template with an extremely large contrast (superhydrophilic/superhydrophobic) for position-controlled growth of CdS nanospheres on TiO<sub>2</sub> nanotube array surfaces. The micropatterned CdS/TiO<sub>2</sub> heterojunction showed a greatly enhanced photocurrent response in both UV and visible light range. These novel nanostructure patterning strategies based on wettability contrast can also be expanded to direct the deposition of other nanostructured materials from aqueous solution. The unique deposition technique paves up new avenues for micro- and nanodevice fabrication.

#### Acknowledgments

The authors thank the financial supports from the National Natural Science Foundation of China (20773100 and 20620130427), National Basic Research Program of China (2007CB935603), the International Scientific and Technological Cooperation Projects of MOST (2007DFC40440), and the National High Technology Research and Development Program of China (2009AA03Z327).

#### Appendix A. Supplementary data

Supplementary data associated with this article can be found, in the online version, at [doi:10.1016/j.matlet.2010.03.017](https://doi.org/10.1016/j.matlet.2010.03.017).

#### References

- [1] Segalman RA. Mater Sci Eng R 2005;48:191–226.
- [2] Kovtyukhova NI, Martin BR, Mbindyo JKN, Mallouk TE, Cabassi M, Mayer TS. Mater Sci Eng C 2002;19:255–62.
- [3] Yang JH, Penmatsa V, Tajima S, Kawarada H, Wang CL. Mater Lett 2009;63:2680–3.
- [4] Francioso L, Siciliano P. Nanotechnology 2006;17:3761–7.
- [5] Zuruzi AS, MacDonald NC. Adv Funct Mater 2005;15:396–402.
- [6] Gao XF, Sun WT, Hu ZD, Ai G, Zhang YL, Feng S, et al. J Phys Chem C 2009;113:20481–5.
- [7] Amos FF, Morin SA, Streifer JA, Hamers RJ, Jin S. J Am Chem Soc 2007;129:14296–302.
- [8] Yoshimura M, Gallage R. J Solid State Electrochem 2008;12:775–82.
- [9] Liu SH, Wang WCM, Mannsfeld SCB, Locklin J, Erk P, Gomez M, et al. Langmuir 2007;23:7428–32.
- [10] Lai YK, Lin ZQ, Huang JY, Sun L, Chen Z, Lin CJ. New J Chem 2010;34:44–51.
- [11] Zhang XT, Jin M, Liu ZY, Tryk D, Nishimoto S, Murakami T, et al. J Phys Chem C 2007;111:14521–9.
- [12] Nishimoto S, Sekine H, Zhang XT, Liu ZY, Nakata K, Murakami T, et al. Langmuir 2009;25:7226–8.
- [13] Lai YK, Lin CJ, Wang H, Huang JY, Zhuang HF, Sun L. Electrochem Commun 2008;10:387–91.
- [14] Lai YK, Lin CJ, Huang JY, Zhuang HF, Sun L, Nguyen T. Langmuir 2008;24:3867–73.
- [15] Lai YK, Gao XF, Zhuang HF, Huang JY, Lin CJ, Jiang L. Adv Mater 2009;21:3799–803.